

Nonzero electric polarization and four magnetoelectric states at zero magnetic field in Cr-doped Y-type hexaferrite

Yongqiang Wang, Shile Zhang, W. K. Zhu, Langsheng Ling, Lei Zhang, Zhe Qu, Li Pi, Wei Tong, Mingliang Tian, and Yuheng Zhang

Citation: *Appl. Phys. Lett.* **110**, 262901 (2017); doi: 10.1063/1.4989999

View online: <http://dx.doi.org/10.1063/1.4989999>

View Table of Contents: <http://aip.scitation.org/toc/apl/110/26>

Published by the [American Institute of Physics](#)

AIP | Applied Physics
Letters

Save your money for your research.
It's now **FREE** to publish with us -
no page, color or publication charges apply.

If your article has the
potential to shape the future of
applied physics, it BELONGS in
Applied Physics Letters

Nonzero electric polarization and four magnetoelectric states at zero magnetic field in Cr-doped Y-type hexaferrite

Yongqiang Wang,^{1,2} Shile Zhang,^{1,a)} W. K. Zhu,¹ Langsheng Ling,¹ Lei Zhang,¹ Zhe Qu,¹ Li Pi,^{1,2,3} Wei Tong,^{1,a)} Mingliang Tian,^{1,3,a)} and Yuheng Zhang^{1,2,3}

¹Anhui Province Key Laboratory of Condensed Matter Physics at Extreme Conditions, High Magnetic Field Laboratory of the Chinese Academy of Sciences, Hefei 230031, China

²Hefei National Laboratory for Physical Sciences at Microscale, University of Science and Technology of China, Hefei 230026, China

³Collaborative Innovation Center of Advanced Microstructures, Nanjing University, Nanjing 210093, China

(Received 10 May 2017; accepted 13 June 2017; published online 27 June 2017)

We report here an enhanced magnetoelectric effect in a Y-type hexaferrite $\text{Ba}_{0.5}\text{Sr}_{1.5}\text{Zn}_2\text{Fe}_{12}\text{O}_{22}$ with Fe^{3+} ions partially substituted by magnetic Cr^{3+} ions (i.e., BSZFCO). The direct magnetoelectric effect is persistent up to 250 K, with the maximal susceptibility of ~ 1309 ps/m at 75 K. More importantly, the pronounced non-zero electric polarization at zero magnetic field and four magnetoelectric states induced by different initial poling fields make it quite unique to serve in a magnetoelectric device. The stability of the direct (inverse) magnetoelectric effect is confirmed by the nonvolatile behavior in response to the cyclically sweeping magnetic (electric) fields. Our studies provide an insight into the nontrivial properties of BSZFCO, which are promising for multiferroic applications. *Published by AIP Publishing.* [<http://dx.doi.org/10.1063/1.4989999>]

Multiferroic materials, with coupled magnetization and electric polarization, have attracted great attention in recent years for potential applications of next-generation functional materials.^{1–5} Since the first discovery of the magnetoelectric (ME) effect in Cr_2O_3 ,⁶ plenty of single-phase systems have been proved to possess ME effects, such as TbMnO_3 ,¹ BiFeO_3 ,² CoCr_2O_4 ,⁵ etc.^{7,8} However, the occurrence of magnetoelectric effects usually requires low temperatures and high magnetic fields, which prevents further development in practical use.^{1,5,9–14} Therefore, intensive efforts have been devoted to searching for new room-temperature multiferroic materials whose electric polarization can be driven by a low magnetic field, i.e., with a large magnetoelectric response.^{9–13,15–17}

Thanks to the helical spin ordering at high temperature and the more insulating nature, hexaferrites become potential candidates to possess the room-temperature ME effect.^{15,17} According to crystal structural constitution, hexaferrites can be classified into six types, i.e., M-type $(\text{Ba}, \text{Sr})\text{Fe}_{12}\text{O}_{19}$, Y-type $(\text{Ba}, \text{Sr})_2\text{Me}_2\text{Fe}_{12}\text{O}_{22}$, Z-type $(\text{Ba}, \text{Sr})_3\text{Me}_2\text{Fe}_{24}\text{O}_{41}$, W-type $(\text{Ba}, \text{Sr})\text{Me}_2\text{Fe}_{16}\text{O}_{27}$, X-type $(\text{Ba}, \text{Sr})_2\text{Me}_2\text{Fe}_{28}\text{O}_{46}$, and U-type $(\text{Ba}, \text{Sr})_4\text{Me}_2\text{Fe}_{36}\text{O}_{60}$, where Me represents divalent metal ions.⁸ Among these systems, the Y-type hexaferrites are of particular interest for their promising multiferroic applications at high temperatures.¹⁷ In 2005, Kimura *et al.* first reported the ME effect in $\text{Ba}_{0.5}\text{Sr}_{1.5}\text{Zn}_2\text{Fe}_{12}\text{O}_{22}$ (BSZFO).⁹ However, the ME effect was only observed below 130 K because of its low resistance, and a relatively high magnetic field was required to induce the electric polarization.⁹ In 2010, Chun *et al.* found that a small proportion of replacement of Fe^{3+} in BSZFO using non-magnetic Al^{3+} (i.e., BSZFAO) can significantly improve the magnetoelectric response, with a ME susceptibility up to 2.0×10^4 ps/m at 30 K.¹² Unfortunately, the room-temperature ME effect was not realized in BSZFAO.

More recently, $\text{BaSrCo}_{2-x}\text{Zn}_x\text{Fe}_{11}\text{AlO}_{22}$ (BSZCFAO, $x=0$ and 0.4) has been reported to exhibit a room-temperature ME effect, and the maximum inverse ME coupling coefficient is 400 ps/m under a bias magnetic field of 13 Oe.¹⁷

Nevertheless, there are still some key issues existing. The stabilization of the magnetically induced ferroelectric phase at zero magnetic field and room temperature is one of the important issues for memory device applications.^{9–13,16} The inverse ME effect (i.e., magnetization controlled by an electric field) is another important issue for information storage, which is however rarely realized in a single-phase multiferroic material.^{17–20} In order to address these problems, it is necessary to try more methods, including the replacement at the Fe site with magnetic ions. The substitution with magnetic ions can definitely modulate the magnetic ordering and further tune the magnetoelectric effect, in view of the strong coupling of the magnetic structure and magnetoelectric effect in this system.^{9,10,12,13,17,21,22} Hence, the magnetic doping would provide a playground to improve the ME effect, especially the feature at room temperature and zero field, and facilitate the understanding of the ME mechanism.

In this letter, we use the magnetic Cr^{3+} ions to partially replace Fe^{3+} ions in Y-type hexaferrite BSZFO. We find that the polycrystalline $\text{Ba}_{0.5}\text{Sr}_{1.5}\text{Zn}_2\text{Fe}_{11.4}\text{Cr}_{0.6}\text{O}_{22}$ (BSZFCO) reveals an enhanced magnetoelectric coupling effect up to 250 K. More importantly, once polarized, the non-zero electric polarization (without magnetic field) is quite stable with time but easily switched by a relatively low magnetic field. In addition, four different poling fields can induce four distinguishable stable magnetoelectric states at 100 K without the bias magnetic field. The stability of the direct (inverse) ME effect is confirmed by the nonvolatile behavior in response to the cyclically sweeping magnetic (electric) fields. All the nontrivial properties make BSZFCO a very promising system to serve in a low-switching-field magnetoelectric device.

^{a)}Authors to whom correspondence should be addressed: zhangsl@hmfl.ac.cn; weitong@hmfl.ac.cn; and tianml@hmfl.ac.cn

Polycrystalline BSZFCO was synthesized by conventional solid state reaction. High-purity powders of SrCO_3 , BaCO_3 , ZnO , Cr_2O_3 , and Fe_2O_3 were weighed in stoichiometry and thoroughly ground, followed by calcining at 950°C for 24 h. The powders were then milled again, pressed into pellets, and sintered in air at 1150°C for 16 hours. Finally, the sample was annealed in an oxygen atmosphere at 900°C for 48 hours to improve the quality. In order to check the crystal structure, powder X-ray diffraction (XRD) was taken on a Rigaku-TTR3 X-ray diffractometer using Cu K radiation. The magnetic measurements were carried out on a Magnetic Property Measurement System, and the electrical measurements were performed on a home-built Multi Measurement System on a Janis 9 T magnet. In order to perform the magnetoelectric measurements, the sample was polished into thin plates ($3 \times 4 \times 0.47 \text{ mm}^3$) and gold was deposited as electrodes. The poling electric field was applied by using a Keithley 2410 sourcemeter, and the magnetoelectric current was collected by using a Keithley 6517B electrometer. The electric polarization (P) was obtained by integrating magnetoelectric current with time.

As shown in Fig. 1(a), the unit cell of BSZFO consists of FeO_6 octahedrons (Oh) and Fe/ZnO_4 tetrahedrons (Td). The magnetic structure can be described by alternatively arranged L and S blocks, where L and S represent large and small magnetic moments,⁹ respectively. The XRD pattern taken for the Cr-doped sample [Fig. 1(b)] is consistent with the space group $R\bar{3}m$,^{13,17} except a minor impurity phase of Fe_3O_4 (marked with red asterisks).²³ However, the existence of tiny Fe_3O_4 would not change our following discussion or conclusions for its low ferroelectric transition temperature (i.e., 38 K).^{24,25} Figure 1(c) shows the magnetization as a function of temperature taken at a field of 100 Oe . We can clearly see that both the zero-field-cooling (ZFC) and field-cooling (FC) curves

have a sharp peak at about 274 K (T_p), indicating a magnetic transition. The sample has a magnetic ground state of the helical spin structure below 274 K , as evidenced by the stepwise increase in $M-H$ curves [inset of Fig. 1(c)] before reaching the saturated magnetization.^{9,10,12,13} A similar feature has been also found in BSZFO and the Al-doped Y-type hexaferrite (and other hexaferrites), in which the magnetoelectric effect is observed below the transition temperature T_p .^{9-13,15,17}

In order to study the magnetoelectric effect in BSZFCO, the magnetoelectric current driven by a magnetic field was measured at different temperatures. The measurement geometry is illustrated in the bottom inset of Fig. 2(a). The sample was first polarized by a poling electric field of $+0.5 \text{ MV/m}$ under a magnetic field of -20 kOe . Then, the poling electric field was turned off at $H = -2 \text{ kOe}$. After a 40-minute short circuit, the ME current was collected with a sweeping magnetic field from -2 kOe to 30 kOe at a rate of 75 Oe/s . Figure 2(a) shows the electric polarization as a function of the magnetic field ($P-H$) at 10 , 100 , and 250 K , obtained by integrating the ME current with time. Two distinct features can be seen in Fig. 2(a). First, the electric polarization reaches its positive maximum at zero magnetic field for $T = 10$ and 100 K . The rectangular-like $P-H$ loop taken at 100 K [top inset of Fig. 2(a)] suggests that the electric polarization is very stable at zero magnetic field, which is important for ferroelectric applications.²⁶ This feature has not been observed in other Y-type hexaferrites.^{9,10,12,13,16,17} BSZFO,⁹ BSZFAO,¹² and BSZCFAO^{13,17} show no/finite electric polarization at zero field, in which the $P-H$ loop is not a rectangle. Second, the direction of electric polarization at 10 and 100 K can be reversed by a small magnetic field. For instance, with the increase in the magnetic field, the electric polarization at 100 K decreases quickly and crosses zero at about 1.2 kOe

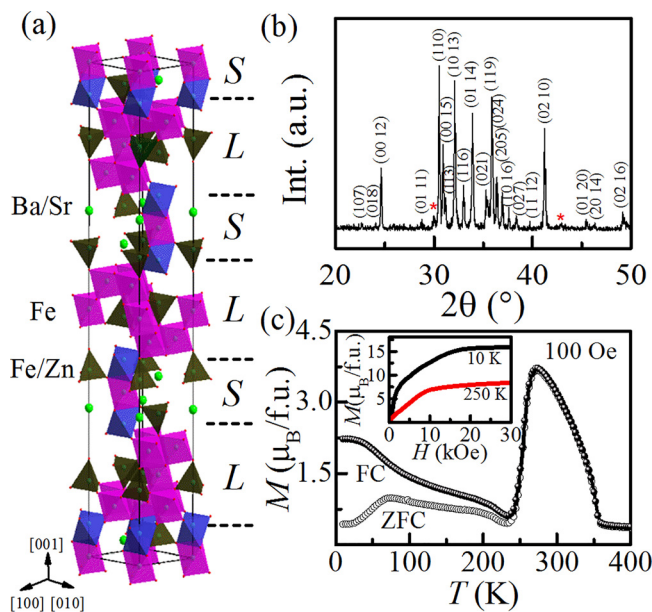


FIG. 1. (a) Crystal structure of $\text{Ba}_{0.5}\text{Sr}_{1.5}\text{Zn}_2\text{Fe}_{12}\text{O}_{22}$. S and L represent the alternative small spin state and large spin state, respectively. (b) Powder XRD pattern of $\text{Ba}_{0.5}\text{Sr}_{1.5}\text{Zn}_2\text{Fe}_{11.4}\text{Cr}_{0.6}\text{O}_{22}$. Red asterisks indicate a minor impurity phase of Fe_3O_4 . (c) Temperature dependence of FC and ZFC magnetization taken at an applied field of 100 Oe . The inset shows the magnetization as a function of the magnetic field at 10 and 250 K .

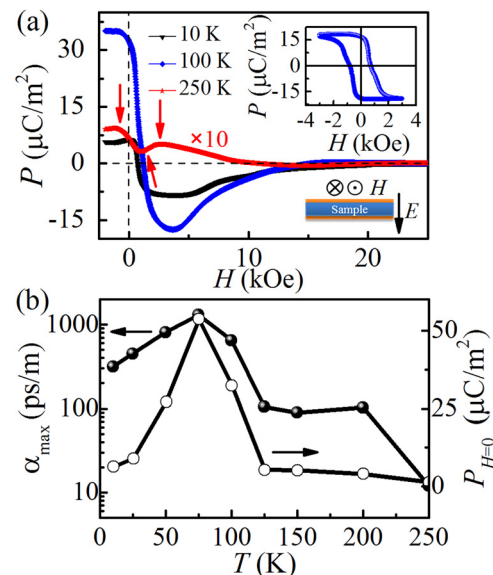


FIG. 2. (a) Electric polarization vs magnetic field at $T = 10$, 100 , and 250 K , obtained by integrating magnetoelectric current with time. Arrows indicate special positions corresponding to a peak or dip. Top inset: $P-H$ loop at 100 K with $-H$ and $+E$ poling fields. The bottom inset shows the measurement geometry. (b) The maximum ME coupling coefficient (left, filled circles) and zero-field electric polarization (right, open circles) as a function of temperature.

and then reaches the negative maximum at about 3.6 kOe. When the magnetic field is further increased, the polarization gradually decays to zero at about 15 kOe, where the magnetic structure enters a collinear ferrimagnetic state [see the inset of Fig. 1(c)].^{9,10,12,13} The change in the sign of electric polarization by a magnetic field is rarely seen in other magnetoelectric hexaferrites,^{11,15} which thus makes BSZFCO a fascinating system to serve in a low-switching-field magnetoelectric device.

The non-zero electric polarization at zero magnetic field extracted from the P - H curves between 10 and 250 K is displayed in Fig. 2(b). While the maximum polarization appears at about 75 K, the ME effect persists up to 250 K. As shown in Fig. 2(a), the P - H curve taken at 250 K exhibits a small dip at about 1 kOe and two extreme points at about -1 and 3 kOe, respectively, which is different from the curves taken at 10 and 100 K. The temperature dependent maximum ME coupling coefficient, defined as $\alpha_{\max} = (\alpha_{\text{ME}} = dP/dH)_{\max}$, is also calculated [Fig. 2(b)], and the maximum α_{\max} occurs at about 75 K (~ 1309 ps/m).

As previously reported, the non-magnetic doping of Al^{3+} ions in BSZFO reduces the in-plane magnetic anisotropy and results in a heliconical spin state, which enhances the low-field ME effect.^{12,21,22} A similar characteristic can be found in $\text{Ba}_2\text{Mg}_2\text{Fe}_{12}\text{O}_{22}$ (BMFO), in which Mg^{2+} partially occupies the octahedral Fe site and reduces the magnetic anisotropy.¹⁰ The magnetic doping of Cr^{3+} ions in BSZFO leads to a switchable polarization by a relatively low magnetic field and a non-zero electric polarization state at zero magnetic field, which is however different from the other Y-type hexaferrites.^{9,10,12,13,17} That is to say, BSZFCO has a different magnetic ground state with respect to the other Y-type hexaferrites. According to the inverse DM-interaction model,²⁷ the electric polarization is zero for a perfect proper-screw or a longitudinal conical magnetic structure, which suggests that the magnetic ground state of Cr-doped BSZFO is not this kind. To clearly understand this, further studies need to be done.

As a result of the non-zero electric polarization at zero magnetic field and the magnetic-field-induced reversible electric polarization, BSZFCO shows great application potential for the next-generation electronic devices. So, the stability or robustness of the ME effect with time becomes more important. Figure 3 presents the electric polarization switched by a magnetic field between ± 3 kOe taken at 100 K. We can clearly see that the electric polarization is reversed by the magnetic field, and the maximum polarization shows almost no decrease, suggesting a nonvolatile feature with time. Besides, with the magnetic field decreasing from ± 3 kOe to zero, the electric polarization remains stable, i.e., showing a large remanent polarization which can be switched by a few hundred Oersteds reversing field. The response of electric polarization is a quite standard rectangular wave, which is convenient for signal processing.

The magnetization controlled by the electric field (M - E), i.e., the inverse ME effect, is another important issue to check. Before taking M - E , the sample was polarized as the following procedure: the poling fields of $H = \pm 30$ kOe and $E = \pm 0.7$ MV/m were first applied, and then, the magnetic field was decreased to ± 2 kOe, and simultaneously, the electric field was set to zero; at last, the magnetic field was set to

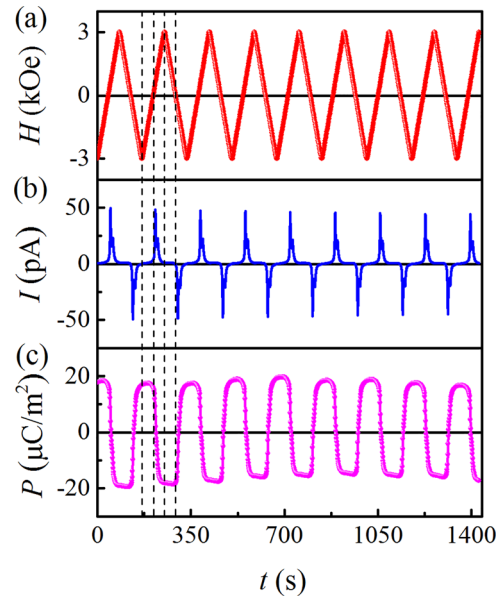


FIG. 3. (a) Oscillating magnetic fields, (b) magnetoelectric current, and (c) switchable electric polarization as a function of time at 100 K. The field sweeping rate is 75 Oe/s.

zero, and after that, the M - E loop was taken by sweeping the electric field between ± 0.7 MV/m. Figure 4 shows the asymmetric butterfly-shape M - E loops (i.e., double loops with the crossing point slightly shifting from the original point) for different initial poling fields. Although small, the remanent magnetization from the hysteresis of the M - E loop at zero electric field is meaningful for a nonvolatile random access memory.^{19,28} In Fig. 4(a), both of the poling fields are set in the positive direction (i.e., $+H$ and $+E$), and hence, the maximum magnetization appears at $+E$ and its sign is plus, while the magnetization at $-E$ is slightly reduced. This fact means that the polarization strongly depends on the initial poling fields, again confirming the robustness of polarization. A similar rule applies for other initial settings of poling fields [Figs. 4(b)–4(d)]. In total, according to different poling fields, four distinguishable magnetoelectric states can be observed at zero magnetic field.

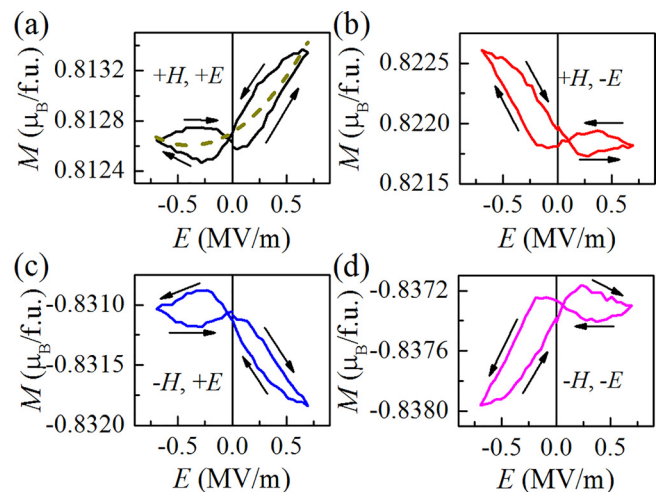


FIG. 4. Electric field dependence of magnetization taken at zero H bias for different poling fields at 100 K. Arrows indicate the direction of the sweeping field ($0 \rightarrow +1 \rightarrow 0 \rightarrow -1 \rightarrow 0$ MV/m). The dashed line in (a) represents the fitting curve with $M(E) - M(0) = \alpha_E E + \frac{1}{2} \gamma E^2$.

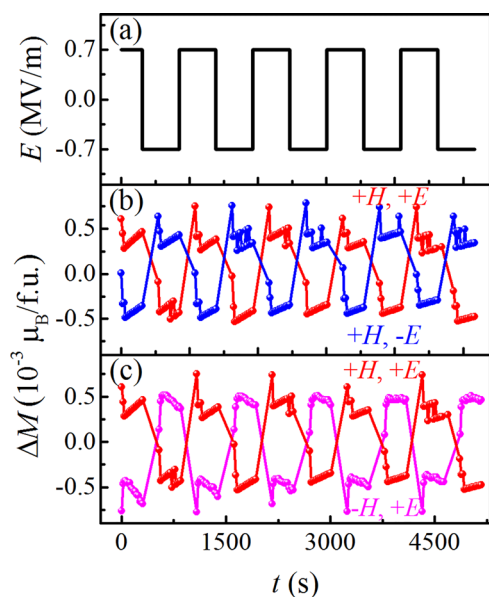


FIG. 5. (a) Pulsed electric field as a function of time at 100 K. (b) and (c) Corresponding magnetization taken at zero H bias for different combinations of initial poling fields ($\pm H, \pm E$), $\Delta M = M(E) - M(0)$. See the text for the initial poling procedure.

The M - E curve in Fig. 4(a) is further fitted to a quadratic function: $M(E) - M(0) = \alpha_E E + \frac{1}{2} \gamma E^2$, where α_E and γ represent the linear and quadratic coefficients, respectively. The resultant quadratic coefficient ($\gamma = 30$ ps/MV) is about three times larger than the linear one ($\alpha_E = 11$ ps/m). This dominant contribution from the quadratic term could be the reason for the asymmetric butterfly-shape loops.¹⁸ These loops are very different from those in BSZCFAO^{17,18} and BSZFAO,²⁰ where the linear coefficient plays a key role in the inverse ME effect and results in a single loop.

In order to check the time stability of magnetization driven by the electric field, the magnetization is then taken by applying a pulsed electric field. The initial poling procedure (curves labeled with $\pm H$ and $\pm E$) is the same as described above. As shown in Fig. 5, with the sign change in the pulsed electric field, the magnetization (measured without the bias magnetic field) changes correspondingly as in Fig. 4. The cyclically varied magnetization seems to have no loss at the maximal value, confirming that the inverse ME effect is also nonvolatile. Another interesting information extracted from Fig. 5 is that the magnetization can always be modulated (with respect to $M(E=0)$) by the pulsed electric field no matter what the initial poling fields are ($\pm H, \pm E$), which would provide a wide platform for possible applications.

In summary, we have found an enhanced ME effect in a magnetic Cr^{3+} doped Y-type hexaferrite, BSZFCO. The direct ME effect is persistent up to 250 K, with a maximal ME susceptibility of ~ 1309 ps/m at 75 K. The non-zero electric polarization at zero magnetic field with low-magnetic-field reversibility makes BSZFCO quite unique to serve in a magnetoelectric device. The stability of the direct (inverse) ME effect is confirmed by the nonvolatile behavior in response to the cyclically sweeping magnetic (electric) fields. Moreover, four different poling fields can induce four distinguishable magnetoelectric states under zero magnetic field at 100 K. Our

studies provide an insight into the nontrivial properties of BSZFCO for promising multiferroic applications.

This work was supported by the National Key Research and Development Program of China (Grant Nos. 2016YFA0401802 and 2017YFA0402900), the Natural Science Foundation of China (Grant Nos. 11304323, 51603207, and U1532153), and the Major Program of Development Foundation of Hefei Center for Physical Science and Technology (Grant No. 2016FXZY001). W. Tong would like to specially thank the Youth Innovation Promotion Association from the Chinese Academy of Sciences.

- ¹T. Kimura, T. Goto, H. Shintani, K. Ishizaka, T. Arima, and Y. Tokura, *Nature* **426**, 55 (2003).
- ²J. Wang, J. B. Neaton, H. Zheng, V. Nagarajan, S. B. Ogale, B. Liu, D. Viehland, V. Vaithyanathan, D. G. Schlom, U. V. Waghmare, N. A. Spaldin, K. M. Rabe, M. Wuttig, and R. Ramesh, *Science* **299**, 1719 (2003).
- ³N. Hur, S. Park, P. A. Sharma, J. S. Ahn, S. Guha, and S. W. Cheong, *Nature* **429**, 392 (2004).
- ⁴B. B. Van Aken, J.-P. Rivera, H. Schmid, and M. Fiebig, *Nature* **449**, 702 (2007).
- ⁵Y. Yamasaki, S. Miyasaka, Y. Kaneko, J. P. He, T. Arima, and Y. Tokura, *Phys. Rev. Lett.* **96**, 207204 (2006).
- ⁶D. N. Astrov, *Sov. Phys. JETP* **11**, 708 (1960), available at <http://jetp.ac.ru/cgi-bin/e/index/e/11/3/p708?a=list>.
- ⁷K. Wang, J.-M. Liu, and Z. Ren, *Adv. Phys.* **58**, 321 (2009).
- ⁸T. Kimura, *Annu. Rev. Condens. Matter Phys.* **3**, 93 (2012).
- ⁹T. Kimura, G. Lawes, and A. P. Ramirez, *Phys. Rev. Lett.* **94**, 137201 (2005).
- ¹⁰S. Ishiwata, Y. Taguchi, H. Murakawa, Y. Onose, and Y. Tokura, *Science* **319**, 1643 (2008).
- ¹¹Y. Tokunaga, Y. Kaneko, D. Okuyama, S. Ishiwata, T. Arima, S. Wakimoto, K. Kakurai, Y. Taguchi, and Y. Tokura, *Phys. Rev. Lett.* **105**, 257201 (2010).
- ¹²S. H. Chun, Y. S. Chai, Y. S. Oh, D. Jaiswal-Nagar, S. Y. Haam, I. Kim, B. Lee, D. H. Nam, K. T. Ko, J. H. Park, J. H. Chung, and K. H. Kim, *Phys. Rev. Lett.* **104**, 037204 (2010).
- ¹³F. Wang, T. Zou, L.-Q. Yan, Y. Liu, and Y. Sun, *Appl. Phys. Lett.* **100**, 122901 (2012).
- ¹⁴S. Shen, L. Yan, Y. Chai, J. Cong, and Y. Sun, *Appl. Phys. Lett.* **104**, 032905 (2014).
- ¹⁵Y. Kitagawa, Y. Hiraoka, T. Honda, T. Ishikura, H. Nakamura, and T. Kimura, *Nat. Mater.* **9**, 797 (2010).
- ¹⁶G. Wang, S. Cao, Y. Cao, S. Hu, X. Wang, Z. Feng, B. Kang, Y. Chai, J. Zhang, and W. Ren, *J. Appl. Phys.* **118**, 094102 (2015).
- ¹⁷S. Hirose, K. Haruki, A. Ando, and T. Kimura, *Appl. Phys. Lett.* **104**, 022907 (2014).
- ¹⁸S. Shen, Y. Chai, and Y. Sun, *Sci. Rep.* **5**, 8254 (2015).
- ¹⁹S. H. Chun, Y. S. Chai, B.-G. Jeon, H. J. Kim, Y. S. Oh, I. Kim, H. Kim, B. J. Jeon, S. Y. Haam, J.-Y. Park, S. H. Lee, J.-H. Chung, J.-H. Park, and K. H. Kim, *Phys. Rev. Lett.* **108**, 177201 (2012).
- ²⁰Y. S. Chai, S. Kwon, S. H. Chun, I. Kim, B.-G. Jeon, K. H. Kim, and S. Lee, *Nat. Commun.* **5**, 4208 (2014).
- ²¹W. S. Noh, K. T. Ko, S. H. Chun, K. H. Kim, B. G. Park, J. Y. Kim, and J. H. Park, *Phys. Rev. Lett.* **114**, 117603 (2015).
- ²²S. Kwon, D. Y. Yoon, S. Lee, Y. S. Chai, S. H. Chun, and K. H. Kim, *Phys. Rev. B* **88**, 064404 (2013).
- ²³M. Wu, X. Gao, Z. Liu, and P. Joy, *J. Am. Ceram. Soc.* **98**, 2498 (2015).
- ²⁴M. Alexe, M. Ziese, D. Hesse, P. Esquinazi, K. Yamauchi, T. Fukushima, S. Picozzi, and U. Gösele, *Adv. Mater.* **21**, 4452 (2009).
- ²⁵M. Ziese, P. D. Esquinazi, D. Pantel, M. Alexe, N. M. Nemes, and M. Garcia-Hernandez, *J. Phys.: Condens. Matter* **24**, 086007 (2012).
- ²⁶J. F. Scott and C. A. P. de Araujo, *Science* **246**, 1400 (1989).
- ²⁷I. A. Sergienko and E. Dagotto, *Phys. Rev. B* **73**, 094434 (2006).
- ²⁸S. Zhang, Y. G. Zhao, P. S. Li, J. J. Yang, S. Rizwan, J. X. Zhang, J. Seidel, T. L. Qu, Y. J. Yang, Z. L. Luo, Q. He, T. Zou, Q. P. Chen, J. W. Wang, L. F. Yang, Y. Sun, Y. Z. Wu, X. Xiao, X. F. Jin, J. Huang, C. Gao, X. F. Han, and R. Ramesh, *Phys. Rev. Lett.* **108**, 137203 (2012).